International Food Research Journal 30(3): 683 - 695 (June 2023)
Journal homepage: *http://www.ifrj.upm.edu.my*

Gel properties of the gum from Chinese quince (*Chaenomeles sinensis*) seeds

Hou, L. X., Miao, W. B., Yao, Y. T., Zhu, Z. D.,
*Liu, H. M., Qin, Z. and Wang, X. D.

College of Food Science and Technology,
Henan University of Technology, Zhengzhou 450001, China

Article history

Received:
9 August 2021
Received in revised form:
30 September 2022
Accepted:
5 December 2022

Keywords

Chinese quince seed gum,
gel properties,
gel strength,
microstructure

Abstract

The effect of pH and different types and concentrations of salt ions on the gel properties of gum extracted from Chinese quince seeds (CQSG) were investigated by analysing the texture, flow behaviour, water-holding capacity (WHC), zeta potential, and thermal and morphological properties of the gels formed by the gum. Results indicated that the pH and different types and concentrations of ions significantly affected the properties and microstructure of the CQSG gels. However, the various conditions had no obvious effects on the gelling and melting temperatures of the CQSG gels. The effects of the tested salt ions on the WHC of the CQSG gels exhibited different patterns. The zeta potential value increased continuously from -45 to -53 mV with increasing phosphorus concentration, while the presence of $CaCl_2$ caused a continuous decrease in the zeta potential from -35 mV (0.2 wt%) to -22 mV (2 wt%). The present work provides fundamental data for designing novel gelling agents based on gum from Chinese quince seeds for use in processed food.

DOI
https://doi.org/10.47836/ifrj.30.3.12

Introduction

Chinese quince (*Chaenomeles sinensis*) is a semievergreen or deciduous tree in the Rosaceae family. Its fruits are used in traditional Chinese medicine (Teng *et al.*, 2010). Since raw fruits are astringent and woody, they are mainly processed into sweets such as jams and fruit liquors, or used as a source of useful materials such as pectic polysaccharides (Liu *et al.*, 2018; Qin *et al.*, 2019). When compared with apple fruits, extracts from Chinese quince fruits have been applied in beverages or candies that are sold with health claims due to high amounts of phenolics (Hamauzu *et al.*, 2005).

Seed is the major by-product of Chinese quince fruit processing. It mainly contains oil and protein; hence, the seed has drawn increasing interest as a novel oilseed resource in recent years (Wang *et al.*, 2017). In addition to oil and protein, gum is also an important functional component present in the seeds of Chinese quince fruits making up approximately 4.0% of the seeds (Wang *et al.*, 2018). The gum extracted from Chinese quince seeds (CQSG) is a heterogeneous polysaccharide composed of xylose (37.1%), glucose (14.0%), arabinose (13.0%), and a high amount of uronic acid (including galacturonic and glucuronic acids) (Wang *et al.*, 2019). It is a hydrocolloid with good water-holding capacity as reflected by its rheological properties, and swelling capacity in an aqueous solution (Wang *et al.*, 2019). It has been shown that CQSG has good potential for application in the food industry as a stabiliser, emulsifier, and thickener. However, these potential industrial applications of CQSG have not yet been extensively investigated.

Meanwhile, increasing attention has been given to the utilisation of natural gum polysaccharides in gel materials for texture control or encapsulation in probiotic, cosmetic, pharmaceutical, and food products (Olorunsola and Adedokun, 2014; Perez-Masia *et al.*, 2015). The gel properties of several types of polysaccharide gums such as konjac glucomannan, flaxseed gum, gellan gum, and kappa-carrageenan have been investigated (Chen *et al.*, 2006). In general, gel-forming biopolymers can be divided into heat- and cold-setting based on the main

*Corresponding author.
Email: liuhuamin5108@163.com

mechanism of gelation, *i.e.*, gel formation induced by either heat or cool (Silva and Rao, 1999). Furthermore, gel biopolymers can be divided into true and weak gels based on macroscopic behaviour (Chen *et al.*, 2006). Knowledge of gel-forming characteristics is necessary for the industrial utilisation of any polysaccharide gum. However, the gel properties of CQSG have not been thoroughly studied, and the mechanism of how it forms gels is not yet fully understood.

Therefore, the objective of the present work was to study the gel properties of the seed gum extracted from Chinese quince fruits, and to determine the influences of various factors on the microstructure and strength of the gels through rheology, thermal analysis, zeta potential measurement, gel strength measurement, and scanning electron microscopy.

Materials and methods

Materials

The seed gum of Chinese quince fruits (CQSG) was prepared in-house following the extraction and purification processes reported previously (Wang *et al.*, 2018). The prepared CQSG contained approximately 31.7% uronic acids, 37.1% xylose, 14.0% glucose, 13.0% arabinose, 2.8% galactose, 1.3% mannose, and 2.2% protein (Wang *et al.*, 2019). All chemicals and solvents used were of chromatographic or analytical grade.

Gel preparation

The various CQSG gels were prepared following the method reported previously with slight modification (Chen *et al.*, 2006). For a typical run, 100 mg of CQSG was dissolved in 10 mL of deionised water with continuous stirring at room temperature until the seed gum fully swelled. For the gels prepared at various pH values, the pH was adjusted by dissolving 0.1 mol/L NaOH or 0.1 mol/L HCl from pH 2 to 12. The amounts of various salts ($CaCl_2$, NaCl, and complex phosphate salts) in the seed gum solution varied from 0.1 to 2%. After preparation, the samples were kept at 4°C overnight to allow the formation of gels.

Rheological measurement

The rheological properties of the various gel samples were evaluated on a Haake MARS rheometer (Thermo Fisher Scientific, Germany) in combination with a cone plate geometry of C35/1° Ti. For each typical run, the gel sample was analysed at 25°C with shear rates ranging from 0.01 to 1000 s^{-1} (Shaari *et al.*, 2017).

Thermal analysis

A Q20-type DSC (differential scanning calorimeter, TA Instrument, USA) was used to obtain the thermal transition temperatures of the samples. Briefly, 20 mg of the sample was placed on an aluminium pan and then hermetically sealed. The sample cell was heated from 10°C to 60, 70, 80, or 90°C with a heating rate of 5°C/min, and then held for 3 min to ensure that the seed gum solution was homogenous. Next, the temperature was lowered to 10°C at a rate of 5°C/min, held for 8 min, and raised again to 90°C at the same rate. At the same time, an empty hermetically sealed pan was subjected to the same treatment as the reference.

Longitudinal compression measurement

A TA XT2i texture analyser (SMS Ltd., England) was used to evaluate the longitudinal compression of the various gel samples. Briefly, cylindrical gel samples (60 mm in height and 80 mm in diameter) were prepared and subjected to compression tests using a TA 11 probe. The test speed was 0.5 mm/s, the deformation was 7.5 mm, and the trigger force was 5.0 g (Salehi and Kashaninejad, 2017). Textural parameters including gel strength and adhesiveness properties were then obtained and recorded.

Zeta potential measurement

Zeta potential was measured with a Zetasizer Nano (Malvern Instruments Ltd., Worcestershire, UK) across the capillary tube. Prior to testing, the seed gum solutions were prepared and filtered through a 0.45 μm filter. The cell temperature was maintained at 25°C. The data were reported as average values of three replicates.

Water-holding capacity measurement

The gel sample was placed into a centrifugal filter unit. After centrifugation at 3,800 rpm for 15 min, the gel was weighed immediately. Then, the WHC of the gel samples was determined and recorded as percentage (%) of gel weight after centrifugation as compared to the weight of the original gel.

Scanning electron microscopy

An HT-7700 scanning electron microscope (SEM, Hitachi, Japan) was used to elucidate the microstructure of the various gels prepared. Briefly, the gel samples were immersed in slush nitrogen, and then lyophilised in a vacuum freeze-drier. The dried samples were transferred onto a microscope stub, coated with gold powder, and then observed using SEM at an acceleration voltage of 3.0 kV and a magnification of 500×.

Statistical analysis

All experiments were carried out in triplicate, and the results were analysed by SPSS 19.0 software (SPSS, Inc., Chicago, USA). Duncan's multiple range tests were used to calculate the differences in means ($p < 0.05$).

Results and discussion

Textural properties

For any gel to be used in food products, the sensory attribute of texture is a key factor in determining consumers' acceptability of the products (Santagiuliana *et al.*, 2018). The textural properties of the CQSG gels produced under various processing conditions are represented in gel strength and adhesiveness, as shown in Figure 1.

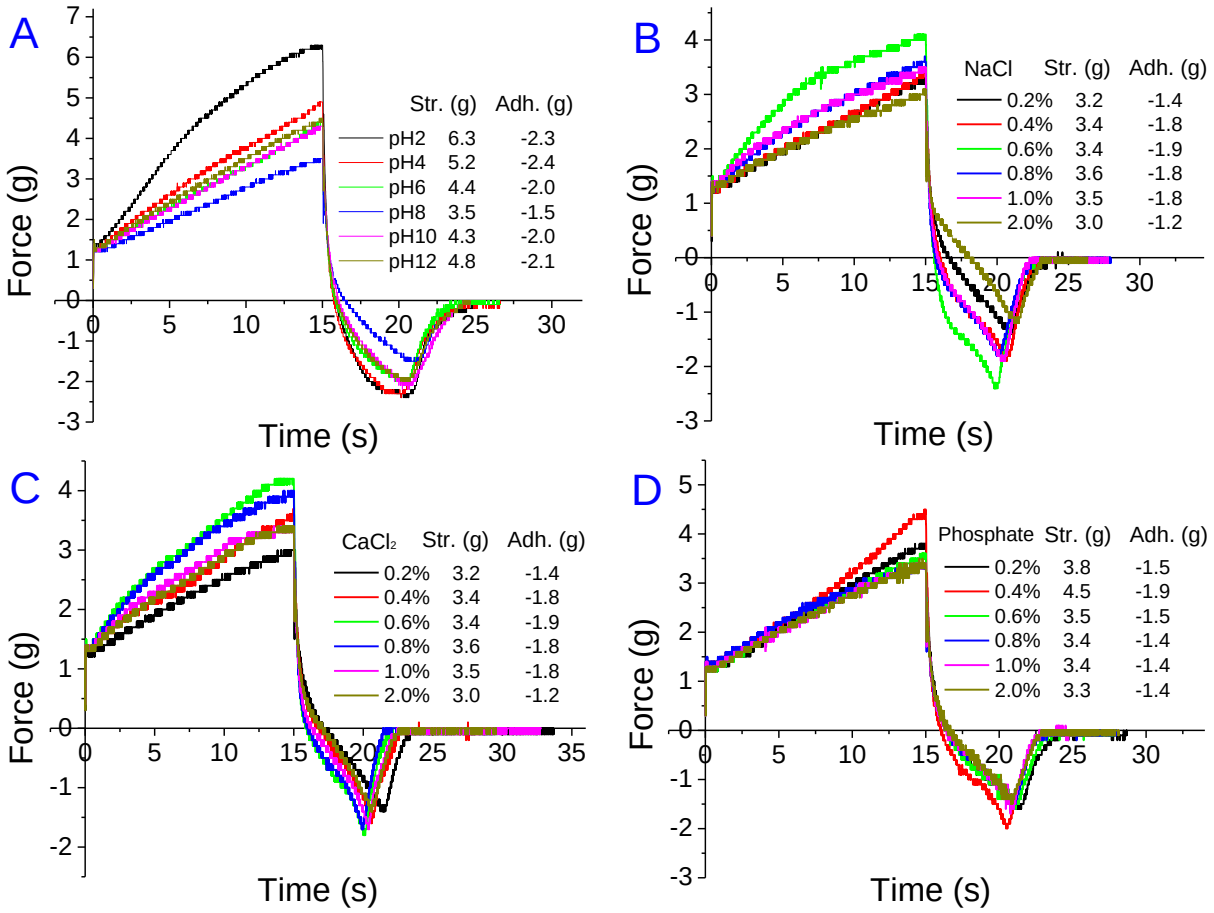

Figure 1. Textural analysis and gel strength of the gels as affected by different conditions.

Gel strength was calculated by determining the force required to break the gel; it indicates a gel's resistance to compression. As shown in Figure 1A, the gel strength of the CQSG gels decreased as the pH increased from pH 2 to 8. Specifically, the gel strength reached a minimum of 3.5 g at pH 8, and then increased to a maximum of 12 as the pH increased. The results showed that pH values influenced CQSG gel strength. CQSG is an anionic polysaccharide that bears a negative charge because of the many ionised carboxyl groups in its molecular structure (Wang *et al.*, 2018; 2019). Intermolecular electrostatic repulsion because of homocharges fully interpenetrates the molecular chains of the biopolymer, thereby inducing the intermolecular cross-linking that results in gelation (Chen *et al.*, 2006). For pH values of 2 - 6, the electrostatic repulsion and hydrogen bonding in the molecular structure of CQSG were very strong. This reduced the ionisation of carboxymethyl in the repulsion which

might lead to the formation of aggregates (Lu *et al.*, 2009; Han *et al.*, 2017). At higher pH values (8 - 12), larger molecules were decomposed into galacturonic acid and other small molecules because of alkaline depolymerisation. In this way, a three-dimensional gelatine network is formed through hydrogen bonding or electrostatic repulsion (Fedeniuk and Biliaderis, 1994).

Adhesiveness measures the resistance of a gel to separation from the probe base; in other words, it indicates the work required to overcome the attractive forces between a gel and a probe surface (Martins *et al.*, 2019). As shown in Figure 1A, adhesiveness was affected by pH. The lowest adhesiveness occurred at pH 8. For most systems, the adhesion mechanism is considered to be a combination of chemical adsorption (the creation of intermolecular primary or secondary bonds between the molecules and adhesive agent on the surface of the adherends) and mechanical interlocking (penetration of adhesive into irregularities or porosities on the adherend surfaces) (Cohen *et al.*, 2013). The gel that exhibited the lowest adhesiveness was at pH 8 because it presented the weakest network structure.

Valence mineral salts are often required in practical applications of hydrocolloids. The physical properties of hydrocolloid gels are influenced by the concentration and type of valence mineral salt (Wu *et al.*, 2018). Therefore, the effect of salt ions on the gel strength and adhesiveness of CQSG gels was investigated. Figures 1B, 1C, and 1D show that CQSG gel strength reached the maximum values when NaCl, $CaCl_2$, and phosphate were at levels of 0.8, 0.8, and 0.4%, respectively. Gel strength decreased when the salt ion amounts increased beyond those levels, especially for phosphate. It is generally known that a specific concentration of salt ions effectively promotes gel formation, whereas excessive salt ions neutralise the negative charges in the gel, thus resulting in the precipitation of the hydrocolloid gum. Excess salt can increase the stability of the gel but will decrease its strength (Thrimawithana *et al.*, 2010). In addition, the different concentrations of the various salt ions had remarkable effects on the adhesiveness of the CQSG gels. The initial addition of the different salt ions led to an increase in adhesiveness, while further increase resulted in a decrease. The CQSG molecules were composed of approximately 29% galacturonic acid (Wang *et al.*, 2019). We expect that the salt ions induced cross-linking between CQSG as this phenomenon is commonly found in pectic polysaccharides (Bemiller and Whistler, 1996). However, the shielding effect of electrostatic repulsion began to dominate as increasing concentrations of salt ions were added. Therefore, the formation of gel networks was inhibited, thus decreasing the adhesiveness correspondingly.

Flow behaviour

The effects of various conditions (pH values and different salt ion types and concentrations) on the flow behaviours of CQSG gels were evaluated by flow measurements under steady-state conditions. The rheological curves are exhibited in Figure 2. As shown, all the gels exhibited pseudoplastic flow. The viscosity decreased quickly as the shear rate increased from 1 to 100 s^{-1}; in contrast, the viscosity of the gel samples decreased slowly at high shear rates from 100 to 1000 s^{-1}. The pH and salt ion concentrations clearly influenced the rheological properties of the gels. To further evaluate the flow behaviour as a function of shear rate, the shear-thinning region of each curve in Figure 2 was fitted to the Ostwald-DeWaele rheological model. The model equation was used to determine the rheological parameters including the flow behaviour index (n), consistency coefficient (K), and coefficients of determination (R^2). The K and n values of all the gel samples are shown in Table 1. As shown, all the samples exhibited high R^2 (ranging from 0.9673 to 0.9998), which indicated that the parameters of the power law model were applicable. The n values indicated closeness to Newtonian flow. $n = 1$ indicates Newtonian flow, and lower n values represent higher degrees of pseudoplastic properties (Pongsawatmanit *et al.*, 2006). The n values were lower than 1 in all samples, thus indicating that all the gel samples were non-Newtonian fluids. When the flow behaviour indices of the gel samples formed at different pH values were compared, lower apparent viscosities were observed for pH 6 and 8. This finding may be correlated with the results of gel strength analysis showing that the gels formed at pH 6 and 8 also had lower strength. Table 1 also shows the K values of CQSG gels with various salt ion concentrations. As shown, the apparent viscosity of the CQSG gels increased at low NaCl and complex phosphate concentrations. The viscosity decreased as the salt ion (NaCl and complex phosphate) concentrations increased. Apparent viscosity analysis indicated that the additional NaCl and complex phosphate had important effects on the

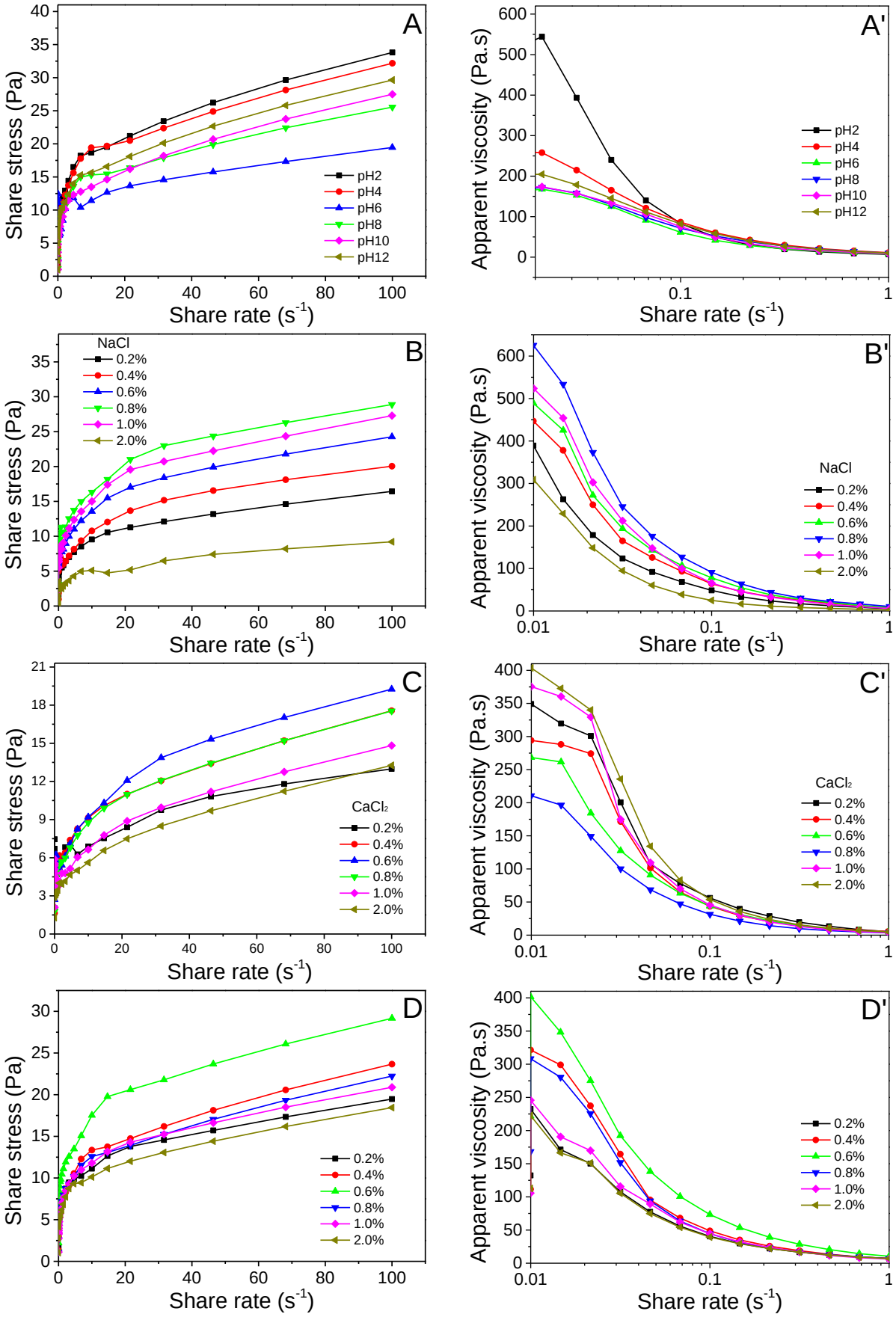

Figure 2. Shear rate dependence of the shear viscosity (A, B, C, and D) and of shear stress (A', B', C', and D') of the gels at various conditions.

Table 1. Rheological parameters of the power law model obtained for the gels under various conditions.

Condition		Rheological parameter			
		τ_0	K	*n*	R^2
Various pH values	2	7.7361	10.6911	0.2000	0.9984
	4	2.2906	9.6752	0.2264	0.9988
	6	0.2588	1.1564	0.5069	0.9872
	8	-0.3019	6.0389	0.2993	0.9816
	10	0.6983	9.1110	0.2582	0.9762
	12	2.1318	9.1372	0.2349	0.9815
NaCl concentrations (w/v) %	0.2%	2.1561	2.0122	0.4385	0.9724
	0.4%	2.6791	3.3078	0.3570	0.9748
	0.6%	4.4817	3.7313	0.3432	0.9821
	0.8%	5.1410	9.6752	0.2000	0.9816
	1.0%	5.0597	4.7822	0.3058	0.9896
	2.0%	-0.3019	0.9377	0.4435	0.9791
$CaCl_2$ concentrations (w/v) %	0.2%	4.46759	1.84953	0.4355	0.9673
	0.4%	3.76020	0.888274	0.5384	0.9864
	0.6%	3.27995	0.528473	0.5992	0.9695
	0.8%	2.67806	0.527908	0.6614	0.9856
	1.0%	4.1944	1.44245	0.5142	0.9835
	2.0%	5.08126	1.94041	0.4336	0.9692
Complex phosphate concentrations (w/v) %	0.2%	0.5522	5.4632	0.2681	0.9997
	0.4%	1.8121	7.37040	0.2487	0.9884
	0.6%	2.0937	8.46731	0.2246	0.9892
	0.8%	1.1341	6.48269	0.2529	0.9797
	1.0%	1.6460	6.13503	0.2569	0.9964
	2.0%	-0.3940	4.63539	0.2683	0.9872

rheological behaviour of CQSG gels. The K values under various $CaCl_2$ concentrations shown in Table 1 demonstrate that there was only a slight decrease in the apparent viscosity of the gels as the $CaCl_2$ concentration increased. In addition, the results showed an increase in the viscoelastic values with increases in $CaCl_2$ concentration. Therefore, the effects of $CaCl_2$ and other tested salt ions on the CQSG gels were different. It is well known that divalent and monovalent cations have different effects on polysaccharide gels. Therefore, to better understand the effect of cations on the CQSG gel and the mechanism of CQSG gel formation, further investigations of the effects of other cations on the CQSG gel are needed.

Water-holding properties

WHC is a pivotal parameter of gel because it influences the sensory quality of gelatinous food; gels with high WHC can better maintain a specific texture of a food. The WHC values of the CQSG gels under various conditions (pH values and different salt ion types and concentrations) were determined, and the results are shown in Figure 3. All tested conditions greatly affected the WHC of the CQSG gels. The WHC of the CQSG gels increased as the pH increased from pH 2 to 6, and then decreased as the pH further increased to 12. The WHC of the CQSG gels increased obviously with increasing $CaCl_2$ and complex phosphate concentrations. The results showed that the WHC of the CQSG gels had a

positive correlation with $CaCl_2$ and complex phosphate concentrations. For the CQSG gels affected by the addition of NaCl, their WHCs first increased with increasing NaCl but then decreased when the added NaCl exceeded 0.4 wt%. The results indicated that the effects of the tested salt ion types on the WHC of the CQSG gels followed different patterns. The WHC of the gels is related to their network microstructure. The cold-set gelation mechanism induced by $CaCl_2$ is different from that of NaCl (Chen *et al.*, 2019). It is well known that the WHC of gels is negatively correlated with the size of the aggregates that are the elementary units of the gels (Chen *et al.*, 2019). Low concentrations of NaCl or low pH may tend to induce CQSG to form a fibrous gel structure, which traps more water. However, further increasing concentrations of NaCl or pH could also cause the gum particles to aggregate rapidly, thereby forming a coarser gel structure. In a coarse gel, WHC is lower because the larger gaps mean a lower capacity to trap water.

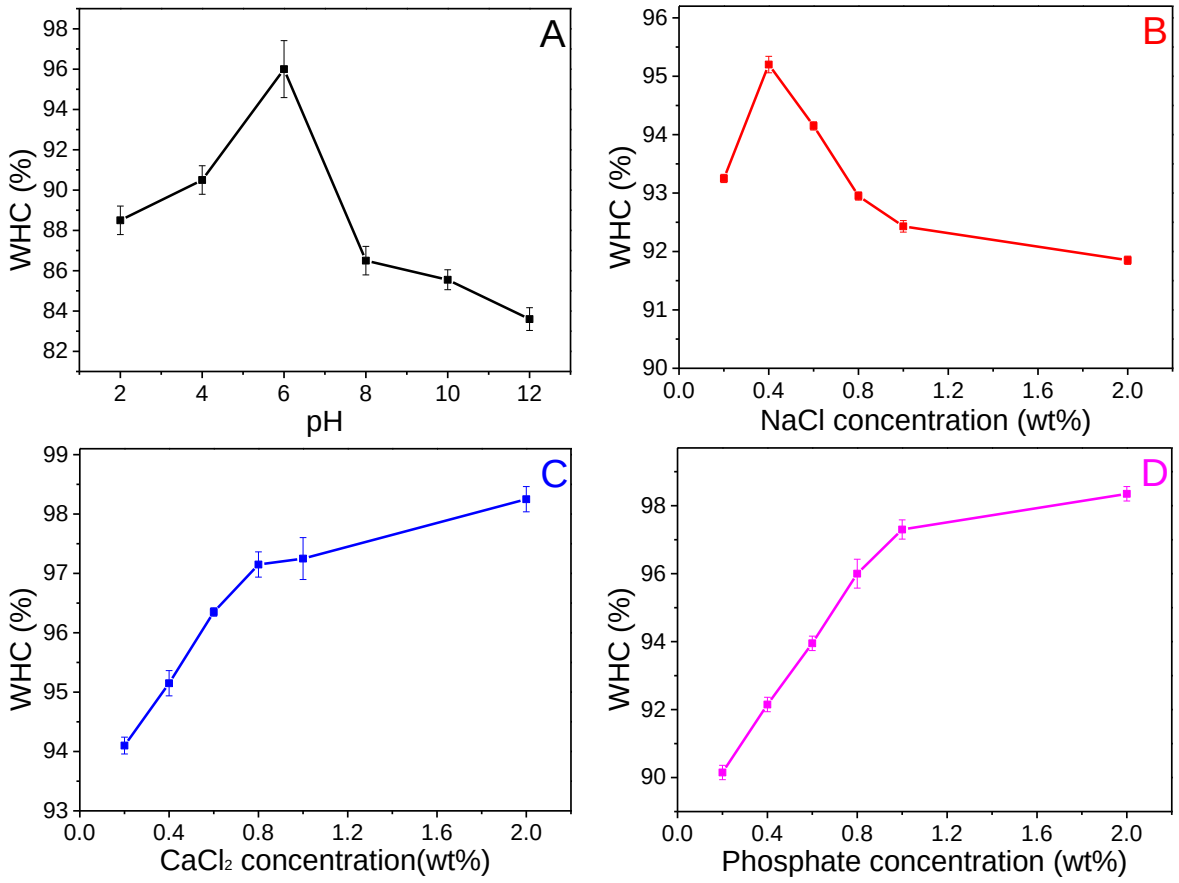

Figure 3. Water holding capacities of CQSG gels under various conditions.

Zeta potential values

Zeta potential value is a scientific term that describes the electrokinetic potential in colloidal systems. This indicates the degree of repulsion between similarly charged particles, and is considered to be significantly associated with the stability of colloidal dispersions (Xiong *et al.*, 2016). The zeta potentials of the CQSG gels under various conditions are shown in Figure 4. Larger values of zeta potential indicate better stability due to stronger mutual repulsion between the electrical double layers of the molecules (Acedo-Carrillo *et al.*, 2006). Smaller zeta potentials indicate that there is little force to prevent macromolecules from coming together. As a general rule, the dividing line between physically stable and unstable systems is ± 30 mV. A system with zeta potentials lower than -30 mV or higher than +30 mV is generally considered stable. As shown in Figure 4A, the zeta potential values of CQSG gels between pH 2 and 12 were below the negative threshold with values from -32 mV at pH 2 to -53 mV at pH 6. There was a further marked increase from -41 mV at pH 8 to -34 mV at pH 12. The decreasing zeta potential as pH increased from 2 to 6 could be attributed to the ionisation of the carboxylic acid in the CQSG macromolecules, while the increasing zeta potential value under alkaline conditions of pH from 8 to 12 could be attributed to the dissociation of carboxyl

groups, thereby reducing the charge density of the CQSG gels (Anvari *et al.*, 2016). The zeta potential of the CQSG gels first increased at low concentrations of NaCl, and then decreased as the concentration increased. The highest value of zeta potential among the NaCl gels was observed at a NaCl concentration of 0.6 wt% (-59 mV). For the phosphate complex, as shown in Figure 4D, the zeta potential increased continuously from -45 to -53 mV with increasing phosphorus concentration. This could be related to the attachment of negatively charged phosphate groups. For $CaCl_2$ gels, the zeta potential decreased continuously from -35 mV (0.2 wt%) to -22 mV (2 wt%), which indicated that the stability of the CQSG gel decreased—and indeed, became unstable—by the addition of $CaCl_2$. The increasing zeta potential value may be due to the association between multivalent cations (Ca^{2+}) and carboxylate groups in the macromolecules of the hydrogel (Pourjavadi and Mahdavinia, 2006) and coordination with -OH groups of the gum (Nasef *et al.*, 2011), thus resulting in the formation of a polyanionic-cationic gel network.

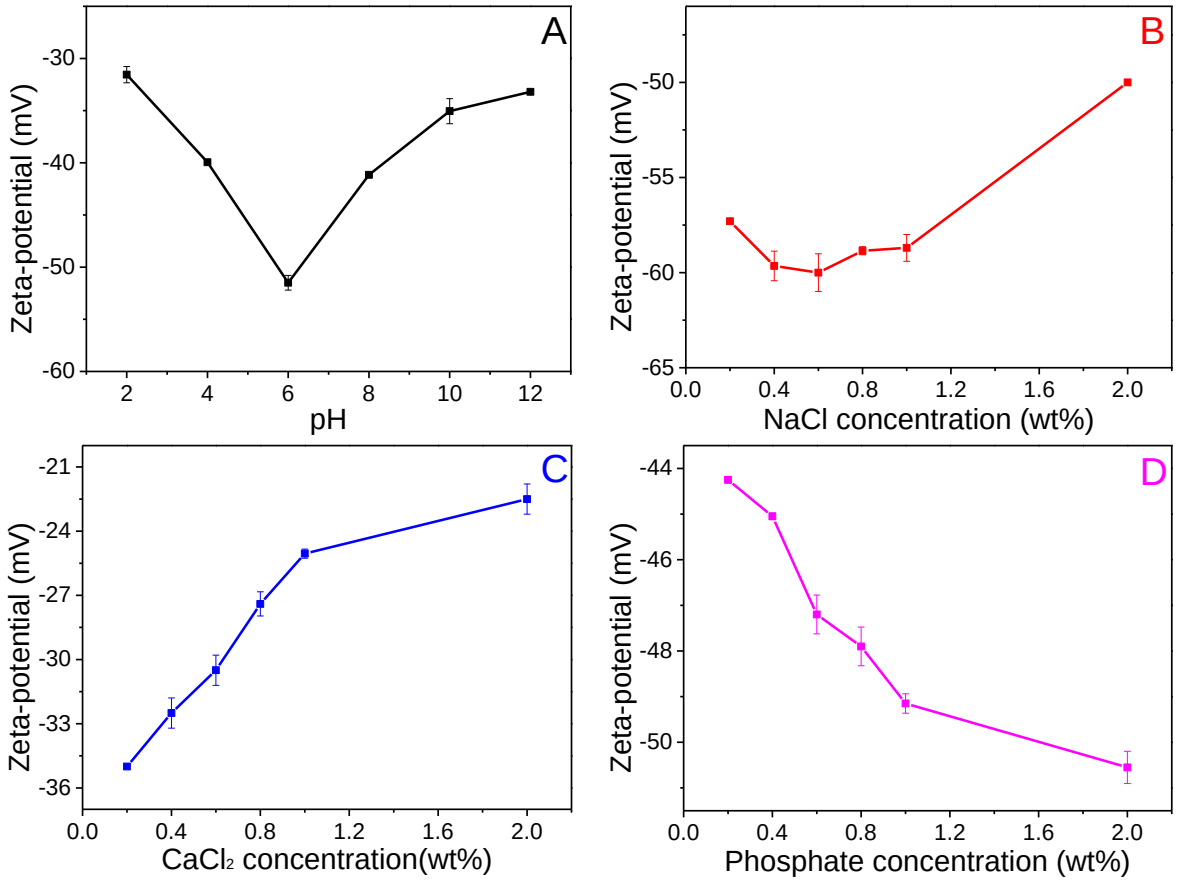

Figure 4. Zeta potentials of the CQSG gels under various conditions.

DSC analysis

The effects of pH and different salt ions and concentrations on the formation of CQSG gels were determined by DSC analysis. The DSC curves are shown in Figure 5. As shown, all the samples distinctly exhibited a single exothermic peak and a single endothermic peak, which indicated that gelling and melting occurred during the cooling and heating processes, respectively. DSC analysis showed that the CQSG gel was thermoreversible; that is, it gels when cooled and melts when heated. The gelling (T_{gel}) and melting (T_{melt}) temperatures of the different CQSG solutions were obtained from the DSC curves, and are shown in Table 2. The reason was that the gelling process and melting process belong to a spontaneously exothermic process and an unspontaneously endothermic process during the gelling and melting processes of food hydrocolloids, respectively (Chen *et al.*, 2006). The interaction that formed networks could not be overcome by thermal energy if the temperature were only raised to T_{gel}. Therefore, extra energy was needed to break the formed network because of the higher T_{melt} when compared with the corresponding T_{gel} (Baeza *et al.*, 2002; Chen *et al.*, 2006). As shown in Table 2, the pH values and the addition of different salt ions at

different concentrations had no large effects on the gelling and melting temperatures of the CQSG gels; however, some slight differences in T_{melt} and T_{gel} for the CQSG gels were observed under various conditions. For example, slightly lower T_{melt} and higher T_{gel} were observed for the addition of 2.0% wt% NaCl when compared with other NaCl concentrations. For the pH 2 sample, T_{melt} was slightly higher than samples at other pH values. The reason for the slight differences in T_{melt} and T_{gel} for the systems containing the highest concentration of NaCl or having a pH of 2 was not clear. Perhaps electrostatic interaction in the macromolecules was involved, thus resulting in changes in the thermal properties of the CQSG gels under those conditions.

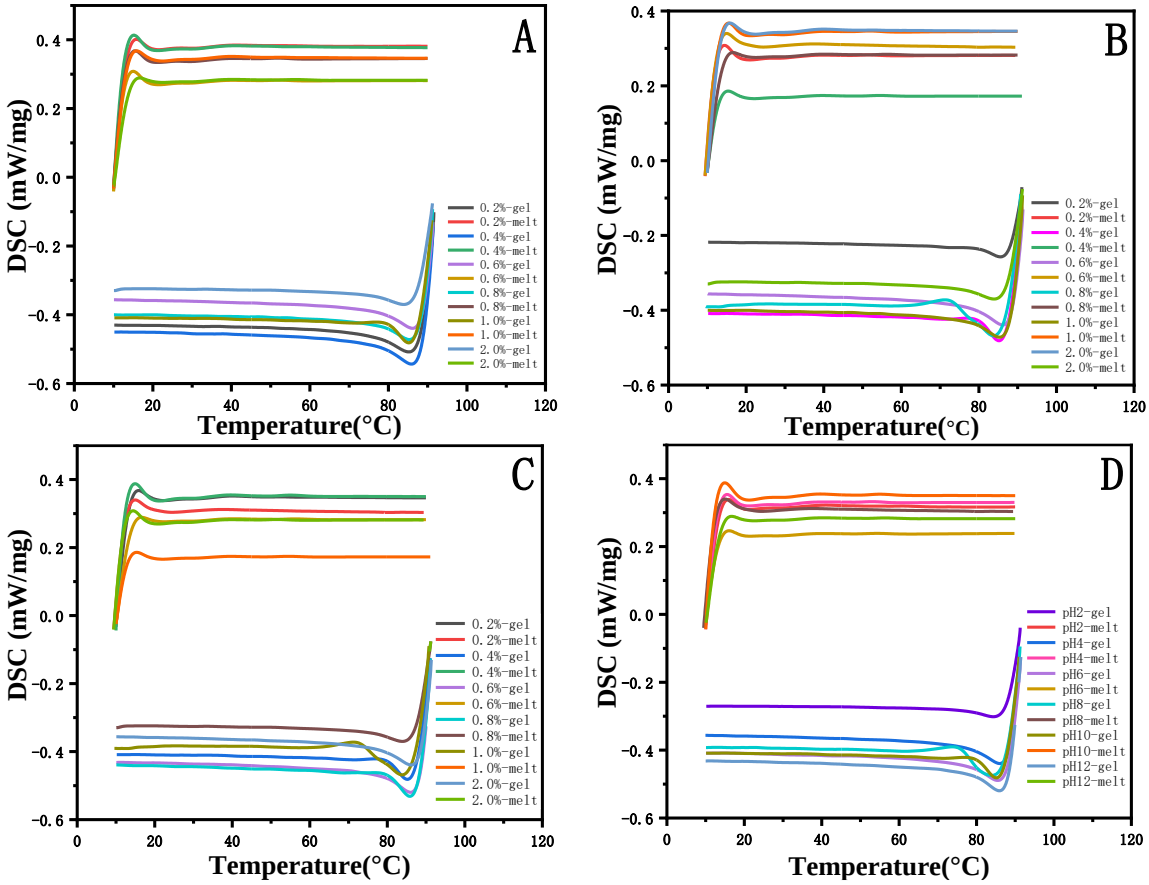

Figure 5. DSC curves for CQSG under different conditions during gelling and melting **(A)** NaCl concentration, **(B)** $CaCl_2$ concentration, **(C)** composite phosphate concentration, and **(D)** different pH values.

Table 2. Effect of pH values and different salt ion types and concentrations on T_{gel} and T_{melt} of CQSG gels.

NaCl (%, w/v)	**0.2**	**0.4**	**0.6**	**0.8**	**1.0**	**2.0**
T_{gel} (°C)	15.82	15.14	15.13	15.32	15.65	16.67
T_{melt} (°C)	85.38	85.98	86.23	85.29	85.11	83.83
$CaCl_2$ (%, w/v)	**0.2**	**0.4**	**0.6**	**0.8**	**1.0**	**2.0**
T_{gel} (°C)	14.4	14.62	14.86	14.95	15.09	15.39
T_{melt} (°C)	85.46	85.90	86.75	85.60	85.20	84.70
Composite phosphate (%, w/v)	**0.2**	**0.4**	**0.6**	**0.8**	**1.0**	**2.0**
T_{gel} (°C)	14.56	14.73	14.94	14.82	14.59	14.34
T_{melt} (°C)	85.77	86.07	86.53	85.18	84.80	84.43
pH	**2**	**4**	**6**	**8**	**10**	**12**
T_{gel} (°C)	16.05	15.93	15.84	15.43	15.68	16.16
T_{melt} (°C)	86.22	85.52	84.88	84.34	84.49	85.11

SEM analysis

SEM is generally used to directly observe the microstructure of dry samples. To avoid any change in the original morphology and structure of the CQSG gels, the samples were freeze-dried at ultralow temperature (-70°C). The SEM observations are shown in Figure 6. In SEM, the fracture plane and the surface of the samples can be observed, thus resulting in images that give a three-dimensional impression because of the depth of field. As shown in Figure 6, the CQSG gels were three-dimensional structures formed with multilayered thin films with large pores. The number and size of pores, and the order of arrangement of the layers of the gels can be used to predict the molecular interactions during gelation. The microstructures of the CQSG gels, as revealed by SEM, differed greatly. Comparing the microstructure of the CQSG gels prepared at various pH values, the network wall was firm and flat at lower pH values (pH 2 and 4), with many fragments or strands linking the network walls. This network structure strengthened the gels which supported the results of textural property analysis. The SEM photographs also revealed that the salt ion type and concentration greatly affected the microstructure of the CQSG gels. When NaCl was added at concentrations ranging from 0.2 to 0.6%, the CQSG gel showed a layered fibrous structure with a porous network between adjacent layers. However, when the NaCl concentration was increased to 2%, the adjacent layers decreased, and the porosity area fraction in the layered structure decreased. In fact, the gel network became filamentous with the aggregation of fine strands in the network. The microstructure of the CQSG gels was related to the water-holding capacity of the gels. A similar phenomenon was also observed in the effect of composite phosphate on the microstructure of the CQSG gels. Comparing the images of other CQSG gels to the image of the gel with the addition of $CaCl_2$, enormous differences were observed in the final gel structures. As shown, the layers of the $CaCl_2$ CQSG gels were thicker than those of the other CQSG gels. By increasing the $CaCl_2$ concentration to 2 wt%, the density of

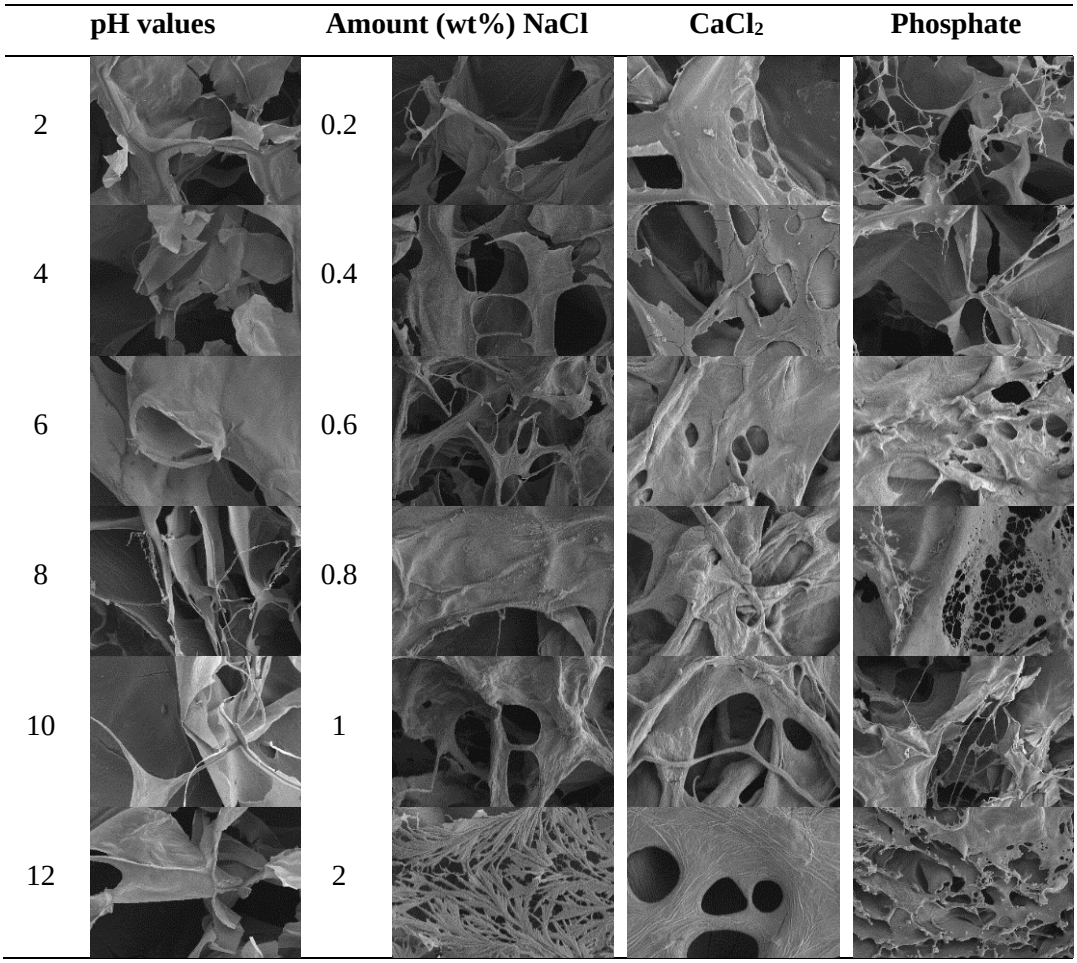

Figure 6. SEM images of the CQSG gels under various conditions after freeze-drying.

aggregation was even greater, thus forming even thicker layers with larger pores. The mechanism of how Ca^{2+} affects the CQSG gel structure is currently unknown; however, one possibility is that calcium ions improve CQSG aggregation, either by changing the conformation of the polysaccharide's molecular chains, or by directly interacting with them to favour aggregation (Guo *et al.*, 2009).

Conclusion

In the present work, the texture, flow behaviours, water holding capacity, zeta potentials, and thermal and morphological properties of the gels formed by CQSG under various conditions were investigated. Different pH values and different salt ion types and concentrations affected these parameters. All the cooling and reheating curves of the DSC analysis exhibited distinct single exothermic and endothermic peaks. The pH values and the addition of different salt ions and concentrations had no obvious effects on the gelling and melting temperatures of the CQSG gels. The WHC of the CQSG gels increased as the pH increased from pH 2 to 6, and then decreased as the pH further increased to 12. The WHC of the CQSG gels had a positive correlation with $CaCl_2$ and complex phosphate concentrations. The effects of the tested salt ions on the WHC of the CQSG gels followed a different pattern. The zeta potential increased continuously from -45 to -53 mV with increasing phosphorus concentration, while the presence of $CaCl_2$ caused a continuous decrease in the zeta potential from -35 mV (0.2 wt%) to -22 mV (2 wt%). These results will be a driving force for the application of CQSG as a novel functional ingredient in the food industry.

Acknowledgement

The present work was financially supported by the Natural Science Foundation of Excellent Youth for Henan (grant no.: 222300420038) and the Key Project of Science and Technology of Henan Province (grant no.: 201300110600).

References

Acedo-Carrillo, J. I., Rosas-Durazo, A., Herrera-Urbina, R., Rinaudo, M., Goycoolea, F. M. and Valdez, M. A. 2006. Zeta potential and drop growth of oil in water emulsions stabilized with mesquite gum. Carbohydrate Molecules 65: 327-336.

Anvari, M., Tabarsa, M., Cao, R., You, S. G., Joyner, M. H. S., Behnam, S. and Rezaei, M. 2016. Compositional characterization and rheological properties of an anionic gum from *Alyssum homolocarpum* seeds. Food Hydrocolloids 52: 766-773.

Baeza, R. I., Carp, D. J., Perez, O. E. and Pilosof, A. M. R. 2002. κ-carrageenan-protein interactions: Effect of proteins on polysaccharide gelling and textural properties. LWT - Food Science and Technology 35: 741-747.

Bemiller, J. N. and Whistler, R. L. 1996. Carbohydrate. In Fennema, O. R. (ed). Food Chemistry, p 157-223. New York: Marcel Dekker.

Chen, H. H., Xu, S. Y. and Wang, Z. 2006. Gelation properties of flaxseed gum. Journal of Food Engineering 77: 295-303.

Chen, X. M., Yuan, J. L., Li, R. X. and Kang, X. 2019. Fabrication, characterization and embedding potential of bovine serum albumin cold-set gel induced by glucono-δ-lactone and sodium chloride. Food Hydrocolloids 95: 273-282.

Cohen, B., Pinkas, O., Foox, M. and Zilberman, M. 2013. Gelatin-alginate novel tissue adhesives and their formulation-strength effects. Acta Biomaterialia 9: 9004-9011.

Fedeniuk, R. W. and Biliaderis, C. G. 1994. Composition and physicochemical properties of linseed (*Linumusitatissimum* L) mucilage. Journal of Agricultural and Food Chemistry 42: 240-247.

Guo, Q., Cui, S. W., Wang, Q., Goff, D. H. and Smith, A. 2009. Microstructure and rheological properties of psyllium polysaccharide gel. Food Hydrocolloids 23: 1542-1547.

Hamauzu, Y., Yasui, H., Inno, T., Kume, C. and Omanyuda, M. 2005. Phenolic profile, antioxidant property, and anti-influenza viral activity of Chinese quince (*Pseudocydonia sinensis* Schneid.), quince (*Cydonia oblonga* Mill.), and apple (*Malus domestica* Mill.) fruits. Journal of Agricultural and Food Chemistry 53: 928-934.

Han, W. Y., Meng, Y. H., Hu, C. Y., Dong, G. R., Qu, Y. L., Deng, H. and Guo, Y. R. 2017.

Mathematical model of Ca^{2+} concentration, pH, pectin concentration and soluble solids (sucrose) on the gelation of low methoxyl pectin. Food Hydrocolloids 66: 37-48.

Lu, L. M., Zhang, L., Qu, F. L., Lu, H. X., Zhang, X. B., Wu, Z. S., ... and Yu, R. Q. 2009. A nano-Ni based ultrasensitive nonenzymatic electrochemical sensor for glucose: Enhancing sensitivity through a nanowire array strategy. Biosensors and Bioelectronics 25: 218-223.

Liu, H. M., Li, Y. R., Wu, M., Yin, H. S. and Wang, X. D. 2018. Two-step isolation of hemicelluloses from Chinese quince fruit: Effect of hydrothermal treatment on structural features. Industrial Crops Products 111: 615-624.

Martins, A. J., Silva, P., Maciel, F., Pastrana, L. M., Cunha, R. L., Cerqueira, M. A. and Vicente, A. A. 2019. Hybrid gels: Influence of oleogel/hydrogel ratio on rheological and textural properties. Food Research International 116: 1298-1305.

Nasef, M. M., El-Hefian, E. A., Saalah, S. and Yahaya, A. H. 2011. Preparation and properties of non-crosslinked and ionically crosslinked chitosan/agar blended hydrogel films. Journal of Chemistry 8: S409-S419.

Olorunsola, E. O. and Adedokun, M. O. 2014. Surface activity as basis for pharmaceutical applications of hydrocolloids: A review. Journal of Applied Pharmaceutical Science 4: 110-116.

Perez-Masia, R., Loeez-Nicolas, R., Periago, M. J., Ros, G., Lagaron, J. M. and Lopez-Rubio, A. 2015. Encapsulation of folic acid in food hydrocolloids through nanospray drying and electrospraying for nutraceutical applications. Food Chemistry 168: 124-133.

Pongsawatmanit, R., Temsiripong, T., Ikeda, S. and Nishinari, K. 2006. Influence of tamarind seed xyloglucan on rheological properties and thermal stability of tapioca starch. Journal of Food Engineering 77: 41-50.

Pourjavadi, A. and Mahdavinia, G. R. 2006. Superabsorbency, pH-sensitivity and swelling kinetics of partially hydrolyzed chitosan-g-poly (acrylamide) hydrogels. Turkish Journal of Chemistry 30: 595-608.

Qin, Z., Liu, H. M., Cheng, X. C. and Wang, X. D. 2019. Effect of drying pretreatment methods on structure and properties of pectins extracted from Chinese quince fruit. International Journal of Biological Macromolecules 137: 801-808.

Salehi, F. and Kashaninejad, M. 2017. Effect of drying methods on textural and rheological properties of basil seed gum. International Food Research Journal 24(5): 2090-2096.

Santagiuliana, M., Piqueras-Fiszman, B., Linden, E. V. D., Stieger, M. and Scholten, E. 2018. Mechanical properties affect detectability of perceived texture contrast in heterogeneous food gels. Food Hydrocolloids 80: 254-263.

Shaari, N. A., Sulaiman, R. and Cheok, C. Y. 2017. Rheological properties of native and modified corn starches in the presence of hydrocolloids. International Food Research Journal 24(5): 2082-2089.

Silva, J. and Rao, M. 1999. Rheological behavior of food gel systems. In: Rao, M. A. (ed). Rheology of Fluid and Semisolid Foods: Principles and Application, p. 319-368. Gaithersburg: Aspen Publishers.

Teng, H., Jo, I. H. and Choi, Y. H. 2010. Optimization of ultrasonic-assisted extraction of phenolic compounds from Chinese quince (*Chaenomeles sinensis*) by response surface methodology. Journal of the Korean Society for Applied Biological Chemistry 53: 618-625.

Thrimawithana, T. R., Young, S., Dunstan, D. E. and Alany, R. G. 2010. Texture and rheological characterization of kappa and iota carrageenan in the presence of counter ions. Carbohydrate Molecules 82: 69-77.

Wang, L., Wu, M., Liu, H. M., Ma, Y. X., Wang, X. D. and Qin, G. Y. 2017. Subcritical fluid extraction of Chinese quince seed: Optimization and product characterization. Molecules 22: 528.

Wang, L., Liu, H. M., Xie, A. J., Wang, X. D., Zhu, C. Y. and Qin, G. Y. 2018. Chinese quince (*Chaenomeles sinensis*) seed gum: Structural characterization. Food Hydrocolloids 75: 237-245.

Wang, L., Liu, H. M., Zhu, C. Y., Xie, A. J., Ma, B. J. and Zhang, P. Z. 2019. Chinese quince seed gum: Flow behaviour, thixotropy and viscoelasticity. Carbohydrate Molecules 209: 230-238.

Wu, Y. B., Ding, W. and He, Q. 2018. The gelation

properties of tara gum blended with k-carrageenan or xanthan. Food Hydrocolloids 77: 764-771.

Xiong, Z. Y., Zhang, M. J. and Ma, M. H. 2016. Emulsifying properties of ovalbumin: Improvement and mechanism by phosphorylation in the presence of sodium tripolyphosphate. Food Hydrocolloids 60: 29-37.